Antenna Technologies for 6G – Advances and Challenges

Y. Jay Guo, *Fellow, IEEE,* Charles A. Guo, *Student Member, IEEE,* Ming Li, *Member, IEEE*, and Matti Latva-aho*, Fellow, IEEE*
(*Invited Paper*)

***Abstract*—This paper presents an overview on the main features and functionalities of the upcoming 6G that have direct implications on antenna technologies. We review the advances of key antenna technologies that are vital to deliver those 6G functionalities with high performance. These include hybrid antenna arrays, analogue multibeam antennas, multiband antenna collocation, reconfigurable intelligent surfaces, reconfigurable antennas, antennas for in-band full duplex (IBFD), mm-wave and THz antennas, wearable antennas and the application of artificial intelligence (AI) to antenna designs. We outline major challenges and, where appropriate, offer potential solutions and research directions.**

***Index Terms*—6G antennas, multibeam antennas, antenna collocation, reconfigurable intelligent surfaces, reconfigurable antennas, IBFD, THz antennas, wearable antennas, ML, AI**

I. Introduction

Driven by emerging applications such as extended reality (XR), holographic communications, and dynamic digital twins (DT) as well as the development of artificial intelligence and high performance computing, wireless communications technologies are experiencing unprecedented rapid growth. Whilst the fifth generation (5G) networks, especially 5G mm-wave systems are still being rolled out, the international standardization body for mobile communications, the Third Generation Partnership Project (3GPP), has already released 3GPP Release 18, known as 5G-Advanced [1], [2], [3]. 5G-Advanced serves as a critical foundation towards future sixth generation (6G) mobile communications networks under the framework of IMT-2030.

Technological evolution from 5G to 6G systems is poised to deliver several key capabilities and features, which is illustrated in Fig. 1, where the key performance indicators of IMT-2030 (6G) and IMT-2020 (5G) are compared, and several of them have significant implications for antenna technologies [4], [5]. First, the expected growth of augmented reality (AR) and virtual reality (VR) as well as dynamic digital twins renders it necessary for future wireless networks to move up to *higher frequency bands* as well as to embrace *massive multi-input-multi-output* (MIMO) to achieve enhanced mobile broadband (eMBB) with unprecedented data rates of up to 1 Tbp/s. Although higher bands are not favorable for large area coverage, they are necessary to deliver the data rates required for certain 6G applications. The massive MIMO concept was first introduced to 5G wireless networks in 3GPP Release 15. By implementing beamforming and spatial multiplexing using antenna arrays with hundreds or even thousands of elements, the system can achieve significant improvement in terms of coverage expansion, increased throughput, and higher signal quality. Moving into 6G, the mobile communications networks are expected to achieve massive MIMO with an even greater number of antenna elements. However, as shown in the current roll-out of 5G, supporting massive MIMO whilst maintaining reasonable base station costs is a significant challenge.

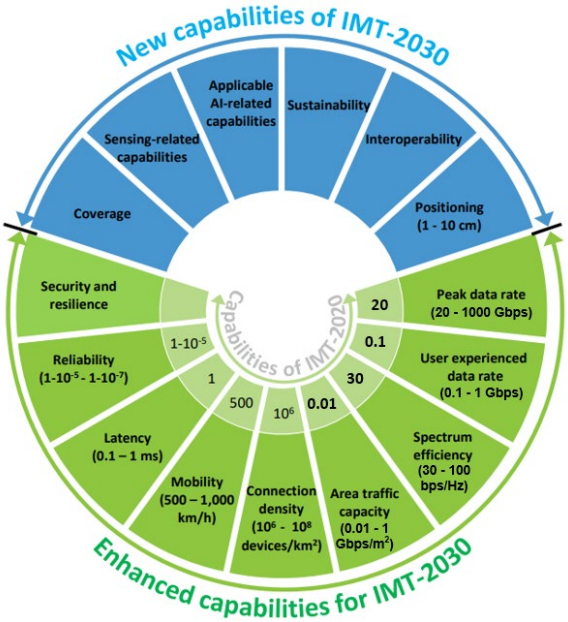

Fig. 1 Enhanced and new capabilities of 6G under the IMT-2030 framework.

Second, integrated sensing and communications (ISAC), which is a variant of joint communications and sensing, is widely regarded as one of the hallmark features of 6G [6], [7]. By exploiting the signatures and changes of radio signals going through the environment, ISAC makes the traditional communications-only network dual-functional, serving as a distributed sensing network whilst supporting connectivity.

Y. Jay Guo and Ming Li are with the Global Big Data Technologies Centre, University of Technology Sydney, Ultimo, NSW 2007, Australia (e-mail: jay.guo@uts.edu.au, ming.li@uts.edu.au).

Charles A. Guo is with the School of Electrical Engineering and Telecommunications, University of New South Wales, NSW 2052, Australia (email: z5280551@ad.unsw.edu.au).

Matti Latva-aho is with the University of Oulu, 90570 Oulu, Finland (email: matti.latva-aho@oulu.fi).

Such a paradigm shift will undoubtedly require new antenna designs, particularly for the base stations. To deliver high-resolution spatial information in a mobile environment, one would need to have steerable narrow beams. Generally speaking, the employment of wide beams and narrow beams would lead to different statistics of the environmental information. In practice, therefore, ISAC would necessitate both fixed wide beams and steerable narrow beams at the base station. Most existing ISAC designs are based on digital arrays. Employing analog arrays or hybrid arrays would provide a low-cost and low-energy-consumption alternative [8].

Third, enhanced sidelink communications that support vehicle-to-everything (V2X), device-to-device (D2D) and machine-type communications are expected to play a key role in a number of industrial applications [9]. This technology will enable direct communications among user terminals (UE) without relying on the core network, aiming to facilitate energy-efficient interactive services like XR and the industrial Internet of Things (IIoT). For example, a vehicle-mounted base station relay can provide services to UEs inside the vehicle or in the vicinity of the vehicle. Furthermore, it is expected that unmanned aerial vehicles (UAVs) will become critical for many industry applications and government services. There, the enhanced sidelink communications technology can be applied to communications among UAVs, and between UAVs and UEs and sensors on the ground. All the above would require dynamic multibeam antenna technologies that can enhance one-to-many connectivity. Due to the constraint on the operation environment of such platforms, it is of paramount importance that the multibeam antenna consumes a minimal amount of energy and is of low cost.

Fourth, the current terrestrial wireless system only serves around 20% of the land area, accounting for 6% of the entire Earth surface. Therefore, the *integration of terrestrial and non-terrestrial networks* (NTN) including UAVs, high-altitude platform station (HAPS), and satellites, will be essential in 6G systems to provide ubiquitous coverage in remote areas and to ensure reliable services during disasters [10], [11]. These new platforms will need new antenna designs that meet their specific requirements. For example, advanced transmitarrays/ reflectarrays are required for LEO satellites to achieve long distance communications whilst facilitating ease of packaging and launch. The non-stationary HAPS would need adaptive multibeams to provide reliable coverage for the intended area. Cost effective LEO satellite and LEO terminal antennas with high gains are needed for people and vehicles on the move. Otherwise, the data rates may remain modest, allowing only messaging for emergency services. Arguably, the most interesting LEO satellite application is direct-to-device services, in which one can use an ordinary phone to connect to LEO satellite for applications of moderate date rates. The most technology challenge to achieve this is a high-gain multibeam LEO satellite antenna with tens of meters in size [12].

Understandably, the standardization of 6G will be mainly at the system level, but it is inevitable that most advanced functionalities and services would require the support of advanced antenna subsystems [13]. In fact, as elaborated in the paper, most new system architectures rely on major advances in antenna technologies to be realized.

This paper aims to provide an overview of the latest advances in antenna technologies for 6G. We shall first discuss some major emerging 6G antenna technologies and their challenges. Then we shall focus on the recent progress of a few selected technologies, including analogue multibeam antennas, multiband collocated base station antennas and the application of AI to antenna designs. Finally, we shed some light on a few broad research directions that may make major impacts on 6G.

II. Key Antenna Technologies

Until 5G, significant efforts had been made to push the frontier of advanced signal processing techniques at the physical layer. For instance, every generation of networks had a hallmark modulation/multiplexing scheme or signal processing technique to significantly increase the spectrum efficiency. Although spectrum efficiency is still a key performance indicator for 6G, an example of which is the potential introduction of the in-band full duplex (IBFD), other metrics such as total energy consumption and cost are becoming more important. 6G antenna designs must meet these requirements. In this section, we outline several key antenna technologies that would form part of the solutions for 6G.

A. Hybrid Antenna Arrays

As was realized in 5G technology development already, all-digital massive MIMO will inevitably lead to very high energy consumption and high manufacturing costs [14], [15]. Consequently, hybrid antenna arrays were introduced to 5G mm-wave base stations by major vendors. A hybrid antenna array consists of both analogue beamformers and digital beamformers [16], [17]. Specifically, analogue beamformers are employed as subarrays and then combined to form a digital beamformer. The analogue subarrays serve to save costs and energy consumption, and the digital beamformer provides a means of intricate signal processing such as beam acquisition and tracking. This way, the complexity of the digital beamformer is reduced by a factor equal to the number of elements in a subarray. The tradeoff between beamforming performance, energy consumption and cost provided by the hybrid array architecture makes it an attractive candidate for certain massive MIMO implementations in 6G. Major challenges facing the antenna community include the difficulties of producing identical phase shifters in broad mm-wave bands, which may cause beam squint that affects system efficiency and reliability, and the losses in phase shifters and the feed network that tend to become more severe at high frequencies. Furthermore, effective support of multibeams in the subarray has not been well addressed from a system point of view in the literature.

B. Multibeam Antennas

To date, sectorization has served as a major technique to increase the system capacity at the base stations [18]. Therefore, the base station antennas have been typically designed to cover some fixed sectors. Moving to 5G-Advanced and 6G, supporting dynamic multiple beamforming will become the

norm. Analogue multibeam antennas can be used in subarrays in a hybrid antenna system, as a feed for a larger antenna or employed alone. These antennas can be designed to have low energy consumption and low cost. In recent years, there has been rapid progress in quasi-optical and circuit-type analogue multibeam antennas [19], [20]. Unfortunately, with just a few exceptions, these antennas are almost exclusively for fixed multibeams. Individually steerable multibeam analogue antennas remain a major challenge. The recently reported Generalized Joined Coupler (GJC) matrix provides a promising solution to individually steerable multibeam antennas [21]. This topic will be elaborated further in Section III.

C. Antenna Collocation

The acquisition of new base station/antenna sites has always been a great challenge to the cellular industry. As a result, antenna collocation has become a common approach in previous generations of mobile wireless networks. The coexistence of antenna arrays working in different bands can have two potential detrimental effects on system performance. The first one is mutual coupling and the second is the cross-scattering between antenna elements of different frequency bands. The cross-scattering of main concern is typically the one caused by lower frequency and therefore larger antennas to the higher frequency smaller antennas, which result in distorted radiation patterns. Since base station antennas are typically designed to provide certain fixed or dynamic angular coverage, such distortion in the antenna patterns need to be suppressed in order to ensure quality coverage; the method to achieve it is called de-scattering [4]. The more bands a base station needs to support, the more difficult de-scattering becomes. Moving to the 6G era, the base stations will need to support the collocation of 6G, 5G, and most likely 4G antennas at the initial phase. Therefore, new wide-band and multibeam de-scattering techniques must be developed. Another challenging issue is for base station antennas to effectively serve UAVs, and LEO satellites whilst supporting mobile users on the ground, see Fig. 2. This demands a paradigm shift in the antenna designs. Antenna collocation will be further discussed in Section IV.

Fig. 2. Base stations supporting UAVs, LEO satellites and users on the ground.

D. Metasurface and Reconfigurable Intelligent Surface (RIS)

A main antenna technology breakthrough in the last two decades is the metasurface [22]. With characteristics not normally found in natural materials, metasurfaces are typically engineered by arranging electrically small scatterers or holes into a two-dimensional pattern at a surface or interface. Metasurfaces have been employed in the design of antennas to increase the bandwidth, shape the beam pattern and generate multibeams [23]. In [24], it was proposed to employ active metasurfaces as reconfigurable antennas with advanced analog signal processing capabilities for future generation transceivers. Another interesting application of metasurfaces is energy harvesting. In [25], an energy collecting metasurface is reported to support ultralow-power wireless communications.

A major application of metasurfaces to 5G and 6G systems is reconfigurable intelligent surface (RIS). The quasi-optical nature of mm-wave and THz waves means that non-line-of-sight (NLoS) propagation would become a major obstacle to establishing communications links. As a result, there has been strong interest in RIS from both academia and industry [13], [26]. Typically, in the form of a metasurface, a RIS can redirect electromagnetic waves toward desired regions. They promise great benefits in not only communications but also localization and mapping in complex NLOS environments. Besides, RISs can provide range extensions in integrated terrestrial and non-terrestrial wireless networks as an alternative to conventional relays, though the latter usually features complex hardware and high power consumption. Although there have been numerous publications in the wireless communications community incorporating massive MIMO in RISs, it is worth noting that, for many if not most applications, RISs need to be of low cost and low energy consumption. Therefore, reconfigurable RISs and hybrid RISs with both passive and active elements may be of greater practicality unless there are major breakthroughs in smart materials that enable low-cost and low-energy beamforming. Furthermore, optically transparent RISs will reduce the effect of large deployment physically and aesthetically. For the above reasons, reconfigurable RIS as a special type of reconfigurable antenna is expected to serve as a major technology for 5G-Advanced and 6G. To this end, a comprehensive review on reconfigurable Huygens' metasurface was reported in [27].

E. Reconfigurable Antennas

Intensive research on reconfigurable antennas has been ongoing for over two decades [28]. Differing from the conventional antennas that are physically fixed once deployed, reconfigurable antennas can change their bandwidth, radiation patterns and polarizations on the fly to deliver optimal system performance, being date rates, communications range or information interceptibility. For the most part, this research has been carried out only in academia [29]. Critical issues hindering the adoption of reconfigurable antennas by industry include the reliability and losses of switches and tunable devices. As an alternative low-loss technology, liquid antennas have been studied since the 1990s. In such antennas, reconfiguration is achieved when antennas reversibly change their geometry,

which then change the operating frequency and beam patterns [30]. Currently, there are still a number of challenges to be addressed to make the solution practical. These include cost, reconfiguration speed, and system complexity and compactness.

From their inception, reconfigurable antennas have been widely considered for use in cognitive wireless systems. Now the advancement toward intelligent 6G networks creates an ideal application space for several types of reconfigurable antennas. These include frequency and beam pattern reconfigurable antennas for applications in moving platforms that require a moderate reconfiguration speed, such as low-cost LEO satellite terminal antennas and UAV antennas, for instance. The reconfigurability feature is expected to be seen in various forms, potentially more for analogue beamforming in both analogue beamformers and RISs, and bandwidth adaptation to support dynamic spectrum allocation.

Recently, a reconfigurable mm-wave dual-polarized antenna array system for future base station antennas was reported. Differing from conventional switching methods, a polarization mixing method was employed to realize wide-range continuous beamwidth control. By simultaneously exciting dual polarizations, the system achieved wider beams, with a continuously adjustable beamwidth ranging from 21° to 100° by only tuning some of the phase shifters without needing any amplitude control [31]. We also extend our consideration of reconfigurable arrays to tightly coupled antenna arrays. An ultrawideband frequency-reconfigurable tightly coupled dipole array was presented in [32]. The design realizes high radiation efficiency and wide beam-scan angles by virtue of a reconfigurable layer and wide-angle impedance matching (WAIM) structure.

Another reconfigurable antenna concept reported recently is movable antennas, which exploit the wireless channel spatial variation in a confined region by enabling local movement of the antennas [33]. Specifically, the positions of antennas at the transmitter and/or receiver can be dynamically changed to obtain better channel conditions for improving the communications performance. However, movable antennas have their inherent limitations such as response speed and difficulty to feed.

F. In-Band Full Duplex

As the demands for connectivity and data rates increase exponentially, there has been a shortage of frequency resources to support new systems, and this spectrum scarcity problem is becoming significantly more severe for 6G. In-band full-duplex (IBFD) technology, which allows transceivers to transmit and receive in the same frequency band simultaneously, is considered as a key solution to the problem of spectrum scarcity [34]. IBFD is also known as simultaneously transmit and receive (STAR) systems [35]. It is also extremely beneficial for joint sensing and communications, as the sensing of the environment can be simply done by directly analyzing the signals scattered from the surrounding environment [7].

A fundamental challenge to IBFD systems is self-interference (SI), which is the signal received by a receiver from a collocated transmitter [36]. SI is significantly stronger than the signal received from an intended distant transmitter. Since the SI in an IBFD system occupies the same frequency band but has much higher power than the desired signal, it must be cancelled first for any receiver to function. To enable an IBFD operation, one would need to sufficiently reduce the SI to below the noise floor, ideally. Typically, the SI power can be anywhere between 70 and 120 dB more powerful than the signal of interest. Worse still, the SI is very sensitive to frequency instability, time variance, nonlinear distortion, and phase noise. These challenges are further exacerbated when cost-sensitive and form-factor-constrained mobile devices are considered.

To effectively cancel the SI, one needs to take a holistic approach to tackle the problem in the propagation/antenna domain, RF domain and digital domain simultaneously. Most recently, we have demonstrated the feasibility of IBFD systems with a state-of-the-art prototype that achieved 75 dB SI cancellation across a 50 MHz band [36]. It employed an adaptive least mean square (ALMS) RF filter with a track/hold function for analogue domain SI cancellation, a pair of decoupled patch antennas for SI mitigation in the propagation domain, and a joint analog and digital SI cancellation scheme.

If separate transmitting and receiving antennas are used, it is straightforward to employ decoupling methods to isolate them [4]. Other methods include employing orthogonal polarizations, orthogonal antenna modes, near-field cancellation and isolation in the feed network [37]. The problem becomes much more challenging when both the transmitting and receiving antennas are closely placed in dual-polarized arrays. Even more challenging is the case when only one dual-polarized antenna array is employed for both transmission and reception. Solutions to these practical antenna configurations serve as great opportunities for future research.

G. MM-Wave and THz Antennas

The rollout of 5G mm-wave starting in the US has spread to other regions including Australia. It has been shown that 5G mm-wave does have the capability of delivering Gigabits/s data rates, serving as an attractive solution for small cells covering data-hungry hot-spots. However, the quasi-optical nature of mm-wave propagation limits the coverage to primarily outdoors, and NLoS coverage proves to be very challenging for open areas without clusters of buildings. For NLoS coverage, it may be necessary to employ reconfigurable intelligent surfaces or other relay devices. In the meantime, 5G mm-wave has served as a great solution to fixed wireless, providing broadband services to homes and offices where there are no wired connections. Moving to 6G, it is expected that some airborne and spaceborne systems will embrace mm-wave and THz. The vast number of airborne systems renders it critical to have low-cost, low energy-consumption, high gain and multibeam mm-wave antennas.

It is worth noting that, in comparison to mm-wave, it is significantly more challenging for THz to be adopted in the 6G timeframe. The current THz power sources and receivers are not mature enough for consumer devices. The propagation

characteristics of THz, including high attenuation loss and susceptibility to weather, make THz systems difficult to serve as an outdoor coverage solution for 6G. Therefore, the current industry consensus is that THz will at best serve as a complementary solution for special applications using quasi-optical antennas [13], [38], [39].

One interesting scenario for sub-THz systems is near-field communications (NFC). When an extremely electrically large THz antenna or RIS is employed, the near-field region can extend to a few hundred meters. This will enable novel applications not possible in the far-field including beyond-Tbps data rates, greatly increased user density, significantly improved security and reliability, and accurate positioning in 3D, etc [40], [41]. How to exploit this potential fully with cost-effective sub-THz transceivers is a challenging task for the antennas, mm-wave and THz research communities.

H. Wearable Antennas

6G promises to provide an immersive communications environment. One 6G use case is personal digital twins, which mirror human biological conditions in a virtual world. This technology will monitor health, behavior, and emotional states, enabling predictive analysis and proactive healthcare interventions. All these will facilitate further proliferation of wearable technologies, which in turn require the development of advanced antennas with attributes aligned with wearables. These attributes include robustness, small size, low weight, high efficiency, high degree of flexibility and low level of radiation exposure to the body [42]. To this end, textile-based materials are growing in popularity as they can be easily integrated into clothing. Transparent antennas represent another promising category, offering seamless integration capabilities with everyday objects such as eyewear [43]. One candidate transparent antenna is the dielectric resonator antenna (DRA). Such a device can be placed on the glass frame or even in the lens region [44].

Although personal digital twins require substantial development to address privacy and security concerns, situational awareness for emergency service and law enforcement personnel presents immediate practical applications [45]. This requires high data rates and ultra-reliable communications, and thus serves as a great use case for 6G. For this type of applications, uniforms provide a natural platform for wearable wireless systems and antennas. The antennas need to support beamforming and be robust.

I. The Application of Artificial Intelligence

Artificial Intelligence (AI), and machine learning (ML) in particular, has undergone significant advancements over the past decade, transforming a wide range of industries. In the realm of antennas, AI is increasingly being employed to optimize complex electromagnetic structures, enhance design precision, and expedite development cycles. In recent years, major efforts have been dedicated to the application of AI to the design of antenna elements, antenna arrays, electromagnetic metasurfaces as well as other structures. Given the challenges to 6G antenna designs, it is expected AI will play an ever-increasing role. A more interesting and more impactful application of AI is its combination with reconfigurable antennas to make the entire wireless system cognitive. These topics will be discussed in Section VI.

For the sake of clarity, the relationship between the key antenna technologies discussed above and the 6G capabilities supported is summarized in Table I.

In the following, we shall delve into a selected number of antenna technologies including analogue multibeam antennas, collocation of multiband antennas for multi-generation cellular systems and the application of AI to antennas. It should be noted that, given that 6G promises a revolution in information and communications systems, one may argue that most current antenna research is relevant. Therefore, the selection of topics only reflects our understanding of the current industry trends and research interests.

TABLE I
KEY ANTENNA TECHNOLOGIES REQUIRED BY 6G CAPABILITIES

Key Antena Technologies	Main 6G Capabilities
Hybrid Antenna Arrays for MIMO	Peak data rate, massive connectivity, capacity, cost reduction, energy saving
Multibeam Antennas	Sensing, coverage, connection density, security, resilience, energy saving
Antenna Collocation	Interoperability, coverage, sustainability
RIS	Coverage, cost and energy saving
Reconfigurable Antennas	Network performance, spectrum sharing, interoperability
In-Band Full Duplex	Spectral efficiency
mmWave and THz antennas	Peak data rate, capacity
Wearable Antennas	Sensing, connectivity, digital twin
Artificial Intelligence as A Design Tool	Energy efficiency, spectrum efficiency, reliability, user experience

III. Analogue Multibeam Antennas

To address the challenge of multiuser communications in future wireless communications and sensing systems, intensive research has been dedicated to analogue multibeam antennas recently. Compared with fully digital beamforming systems, analogue multiple beamforming techniques have the potential to substantially save energy and fabrication costs. Analogue multiple beamformers can be classified into circuit-type multibeam antennas and quasi-optical multibeam antennas [19], [20]. In practice, it might be necessary to combine the two technologies together to meet system specifications.

A. Circuit-Type Multibeam Antennas

The circuit-type multibeam antenna employs a radio frequency circuit as an analogue multiple beamforming network (BFN). Conventional BFNs include the Butler matrix, the Blass matrix and the Nolen matrix. Butler matrices are parallel BFNs that produce orthogonal beams in the sense that the direction of each beam centre aligns with the nulls of all other beams [46]. Although all the beams can be rotated together, for most practical purposes, these beams are fixed. As a result, Butler matrices have found wide applications in base

station antennas to provide sectorization in 3G and 4G systems [18]. The Blass matrix is a series rectangular matrix that can generate multibeams in arbitrary directions [47]. Owing to the perceived low efficiency due to the employment of matched loads on two sides, the beamforming flexibility offered by the Blass matrix has not been taken advantage of until recently [48]. Recent work on the generalized joined coupler (GJC) matrix demonstrated that the losses in a Blass matrix can be minimized by the optimal design of the directional couplers [49], [50]. The Nolen matrix is a lossless variant of the Blass matrix in which all the directional couplers below the diagonal are removed [51]. Consequently, all the matched loads at the end of feeder lines in a Blass matrix are also removed [52].

Currently, serious research efforts are being made to address a number of technical challenges in order to turn analogue BFNs into mainstream 6G technologies. The first challenge is bandwidth, which is particularly important for the Blass matrix and the Nolen matrix. The Blass matrix and the Nolen matrix are effectively series-fed feed networks. Consequently, the effect of deviation from the centre frequency and imperfection in the couplers and phase shifters accumulates along the paths of the signal flow. Furthermore, the use of fixed phase shifters necessarily results in beam squint across the operating band. In theory, as long as each component in a BFN has wideband S parameters and is well matched, circuit-type BFNs can achieve a wide operating bandwidth. In this regard, several wideband BFNs have been reported. An early broadband Nolen matrix in substrate integrated waveguide (SIW) technology is described in [53]. In this work, broadband operation is achieved with adequate coupler delay compensation, resulting in a more parallel matrix topology. The SIW couplers and phase shifters of a 4×4 Nolen matrix are designed at 77 GHz to achieve 11.4% system bandwidth for radar applications. Based on a transformer-based coupler with high isolation between sum and difference ports, a new design approach for developing hybrid couplers with arbitrary power division and broadband phase difference is presented in [54]. Based on this model, a modified coupler is developed by including two L-shaped networks to produce constant phase differences at two output ports. Slotlines and microstrip-to-slotline transitions are used for expanding the bandwidth and introducing a 180° phase difference at the difference port. Based on this design, a simplified wideband 3×3 Nolen matrix is designed utilizing only three hybrid couplers and no phase shifters, reaching over 40% bandwidth,

Recognizing the fact that phase slope alignments between internal components is a major limiting factor for wideband operation of Nolen matrices, an analytical design method based on signal flow graphs and complex exponential signal is proposed in [55]. By virtue of this method, rigorous relationships of phase slope alignments between couplers and phase shifters within the operating band in the traditional 4×4 Nolen matrix topology are derived, and a novel 4× 4 Nolen matrix topology composed of couplers and differential phase shifters with specific phase difference slopes is reported. A 4× 4 Nolen matrix based on the proposed topology centered at 1.8 GHz realized over 40% bandwidth.

The second challenge to analogue BFNs is the large footprint due to their layout and the employment of a large number of components. To ease the problem, phase shifters are integrated in the design of couplers to reduce the component count and make the design more compact in [56]. Another approach to reducing the footprint of analogue BFNs is to employ reconfigurable structures. To this end, it was proposed to increase the number of beams supported by a Nolen matrix by cascading it with a phase shifter network [57]. In this design, each phase shifter between a Nolen matrix output and the antenna is replaced by M phase shifters controlled by a single-pole multi-throw (SPMT) switch. More beams can be produced by using different phase shifters. Consequently, the number of beams produced by the reconfigurable Nolen matrix is increased by M-fold. The large footprint issue can be further resolved by using a multi-layer configuration. Multilayer configuration is particularly suited for stripline and substrate integrated waveguide structures as these structures are closed and stacking them upon one another would cause minimum impact on the transmission performance.

The third challenge to conventional BFNs is the ability to independently steer multibeams. The Butler matrix, the Blass matrix and the Nolen matrix are more suited to support fixed beams. One could introduce switches to these matrices to enable beam switching [57], but beam switching is not the same as beam steering. In theory, one could also steer the beams created using the Blass matrix and the Nolen matrix but, since these beams are interdependent, one would need to change all the phase shifter values associated with all beams in order to just steer one beam. This would lead to excessively complex circuit to control all the phase shifters.

To address this challenge, a new BFN known as the generalized joined coupler (GJC) matrix was introduced as shown in Fig. 3 in the form of the Nolen-like GJC matrix [21]. The other form is the Blass-like GJC matrix. In the GJC matrix, the phase shifters for each beam are placed in such a manner that every row of phase shifters have the same phase shift value so they can be controlled by one common voltage, and each beam can be steered independently with negligible effect on other beams. A theoretical framework is introduced in [49] for synthesizing optimal beams to obtain low sidelobes and nulls as shown in Fig. 4. Although GJC matrices are not lossless as some matched loads are employed in general, it has been demonstrated that high transmission efficiency and reception efficiency can be obtained by particular design choices [49], [50]. It is further revealed that, for the Blass-like GJC matrix, one can obtain deterministic or exact solutions to the coupling coefficients for any given amplitude distribution for exciting multibeams [58]. A special case is orthogonal beams that are similar to those generated by the Butler matrix but with much reduced circuit complexity.

The fourth challenge to analogue BFN technologies is two-dimensional (2D) beamforming. Most reported work on circuit-type BFNs has been focused on one-dimensional (1D) designs. In practice, many applications would need 2D antenna arrays with a wide scanning range. If multibeams are required only in one dimension, one can use a 1D BFN to feed

a 2D array with each BFN port supporting a linear array. As an example, a Nolen matrix operating at 26 GHz (25.25–26.75GHz) using E-plane rectangular waveguides (RWs) is reported to support a 7 × 9 slot array in [59]. The all-metal structure leads to 80% mean efficiency.

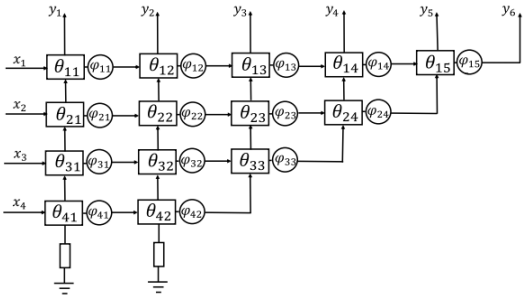

Fig. 3. Illustration of a 4×6 Nolen-like GJC matrix [49].

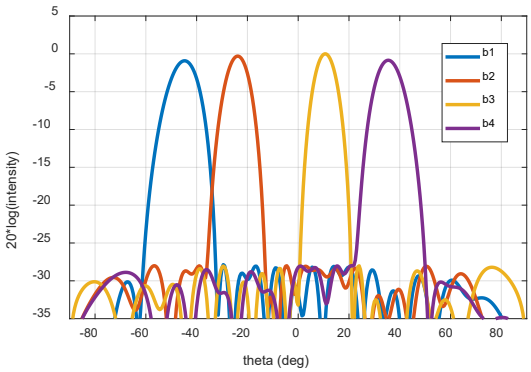

Fig. 4. Beam patterns generated by a 4×16 Nolen-like GJC matrix.

For 2D beamforming, a 2D BFN is required. The classic topology for 2D BFN consists of two sets of sub-BFNs orthogonally connected to each other; they can realize beamforming in both the horizontal and vertical planes. A 2D 3×3 Nolen matrix for 2D beamforming is presented in [60], see Fig. 5. The Nolen matrix is designed by stacking and cascading six 3×3 1D Nolen matrices, and a 2-D patch antenna array is integrated with the 2D Nolen matrix to generate nine radiation beams with unique discrete directions in the azimuthal and elevation planes. The design was realized in microstrip technology operating at 5.8 GHz.

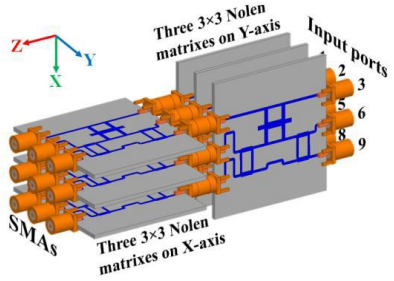

Fig. 5. The schematic of a 3×3 2D Nolen Matrix [60].

The stacking and cascading configuration used in traditional 2D BFNs as shown in Fig. 5 results in a nonplanar topology with a bulky size. To address this issue, a dimension expansion method is proposed in [61]. By using the method, the traditional 2D BFN topology is planarized. The reported planar 2D Nolen matrix as shown in Fig. 6 achieved 50% bandwidth at 1.8 GHz. Similar configurations to the above can also be applied to 2D GJC matrices.

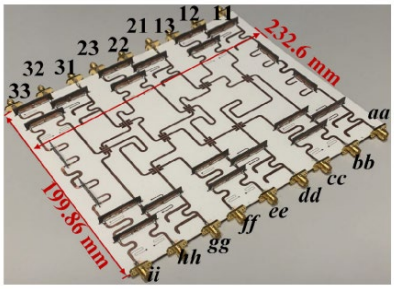

Fig. 6. A planarized 3×3 2D Nolen matrix [61].

It should be noted that there are inherent losses in analogue BFNs in the constituent components such as phase shifters, couplers and transmission lines. Therefore, we envisage they will be used either alone for low-to-intermediate gain antennas where the number of antenna elements and the matrix dimensions are moderate, or as a feed for a quasi-optical antenna. The quasi-optical antenna would provide the gain enhancement for long-range communications.

B. Quasi-Optical Multibeam Antennas

In comparison to circuit-type multibeam antennas, quasi-optical multibeam antennas can achieve much greater gain with high efficiency. Quasi-optical antennas can be in the form of dielectric lenses and metal reflectors, and transmitarrays and reflectarrays [19]. In the following, we shall delve into multibeam lens antennas, multibeam transmitarrays and parallel plate antennas as they do not incur blockage issues caused by multibeam feeds.

1) Multibeam Lens Antennas

High-gain quasi-optical multibeam antennas require multiple feeds or an array to excite them. Lens antennas have the advantage of avoiding the blockage caused by the feed and therefore serve as attractive candidates for 6G systems. Early lens antennas were too heavy and too difficult to fabricate for most microwave and mm-wave applications. In the last decade, the development of metamaterials, artificial materials in general, 3D printing, as well as transformation optics has led to a strong research interest in lens antennas. In particular, owing to its inherent nature of supporting multibeams, the Luneburg lens has received very strong research and industrial interest [62], [63], [64], [65], [66]. Various schemes have been invented to reduce the weight of Luneburg lenses whilst maintaining high efficiency. In [62], for example, a Luneburg lens constructed from planar layers of light-weight cubic foams with conducting inclusions of different sizes placed on a 3D orthogonal grid is reported, see Fig. 7. This method simplifies the manufacture of the lens and reduces its cost and weight which has been a major problem with the Luneburg lens in the lower frequency microwave bands.

Taking advantage of 3D printing, a parallel-plate Luneburg lens based on all-metal metamaterial is presented in [63]. To achieve the required refractive index distribution of the

Luneburg lens, an all-metal unit cell with a separated cuboid is presented, see Fig. 8. The height of the cuboid is determined by the corresponding refractive index. Compared with the traditional bed of nail design, the proposed metamaterial unit cell exhibits a wider bandwidth.

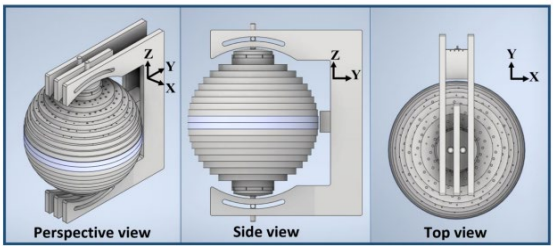

Fig. 7. Illustration of a microwave Luneburg lens antenna made of light artificial material [62].

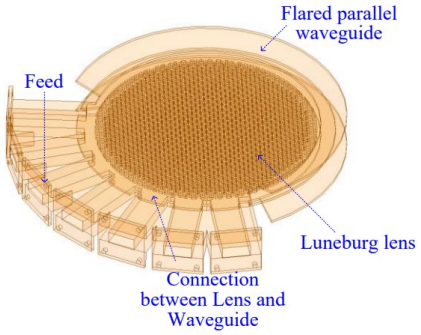

Fig. 8. An all metal 2D Luneburg lens antenna [63].

Another all-metal series dual-fed continuous transverse stub (CTS) array that enables multibeam operation at K-band is reported in [65]. The antenna employs a reflecting Luneburg lens beamformer made of two stacked circular parallel plate waveguides (PPWs). The bottom PPW hosts a graded index medium that collimates the rays coupled by a corner reflector to the top PPW, where the CTS array is located. This design capitalizes on the rotational symmetry of the Luneburg lens, using a circular array of feeds to generate multiple planar wavefronts that illuminate the CTS array across a 360° range. Then, a new series-fed CTS array is introduced to ensure high aperture efficiency.

There are challenges in employing the Luneburg lens for practical multibeam applications as, in the shape of a sphere, the Luneburg lens is bulky. The sphere shape also makes it difficult to excite a Luneburg antenna with a compact feed. As a result, many reported designs have a large footprint for the network. An interesting approach is taken in [66] to address these two challenges simultaneously. In this work, a Terahertz half-compressed elliptical Luneburg lens is designed based on transformation optics. It first compresses the sphere into an ellipse to lower the profile of the Luneburg lens and then compresses the ellipse further into a half ellipse to accommodate a planar feed.

Another approach to lowering the profile of a lens is to employ flat gradient refraction index (GRIN) lenses [67]. In [68], a 2D multibeam GRIN lens antenna with 66.4% aperture efficiency is reported, see Fig. 9. Subwavelength triple-metal-layer unit cells are designed to emulate the local refractive indices. A 2D multibeam GRIN lens, fed by 13 modules of 2×2 patch arrays displaced along *xoz* and *yoz* focus loci, was successfully designed, see Fig. 9. Wide-angle multibeam radiations are obtained with a beam coverage of around ±45° in both the *xoz* and *yoz* planes. The multibeam radiation patterns are stable in a 22.2% bandwidth from 12 to 15 GHz. Unfortunately, one drawback of this design is that the locations of the feeds are on circular arcs. Further research is thus needed to create planar structures to lower the overall profile of the antenna system.

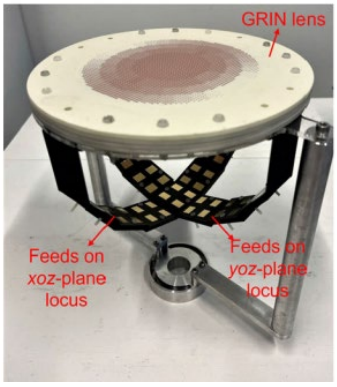

Fig. 9. A multibeam GRIN lens antenna [68].

2) *Multibeam Transmitarrays*

In contrast to lenses and reflectors, transmitarrays offer the advantages of low profile, light weight and greater flexibility to create different beams. They can also be made conformal to suit a nonplanar platform [69]. Their design techniques are based on phased arrays and spatial electromagnetic (EM) wave manipulation. The surface typically comprises a large number of unit cells. These unit cells are designed to compensate for spatial phase delays from the feed, and to provide amplitude modulations, thus beamforming in specific directions with desired beam shapes. Most reported transmitarrays are designed to support one single fixed beam, though more recent research has progressed to support beam steering. By incorporating tunable components into unit cell geometries for dynamic phase control, one can produce a reconfigurable transmitarray to support beam steering [27], [70], [71]. Other efforts have been made to design unit cells that have broad bandwidth and high transmission efficiency [72].

In [73], a wideband and high-gain multibeam array antenna is reported, which is comprised of a Rotman lens and a parallel-fed slot antenna array as the feed, and a Huygens' metasurface, see Fig. 10. The wideband Huygens' unit cells employed are based on dual-offset electric dipole pairs. Differing from traditional designs using a combination of electric and magnetic polarizabilities, the reported Huygens' unit cell exclusively employs electric polarizabilities. As a result, it mitigates the occurrence of unbalanced resonant frequencies between the two polarizabilities, thereby achieving wideband transmission. Based on the proposed unit cell, a wideband and high-gain multibeam array antenna is developed. Without using a series-fed slot antenna array, the multibeam array antenna operates within a relatively wide bandwidth (28–32 GHz).

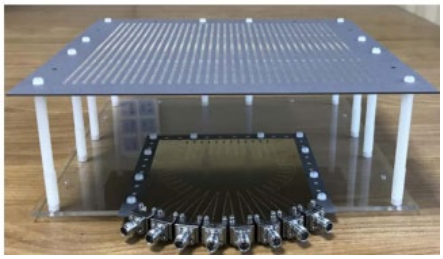

Fig. 10. A Huygens metasurface fed by a Rotman lens excited array [73].

A thin transmitarray can be easily curved to make it conformal. As an example, a transmitarray antenna with an elliptical cylindrical shape is presented for producing wide-angle multibeams in [69]. The transmitarray has a cylindrical radiating aperture with an elliptical cross-section, as shown in Fig. 11. Multiple feeds can be placed on the middle horizontal plane to realize multiple beams. Inspired by the 2D Ruze lens, the antenna shape and the phase compensation are jointly designed according to the desired maximal beam direction.

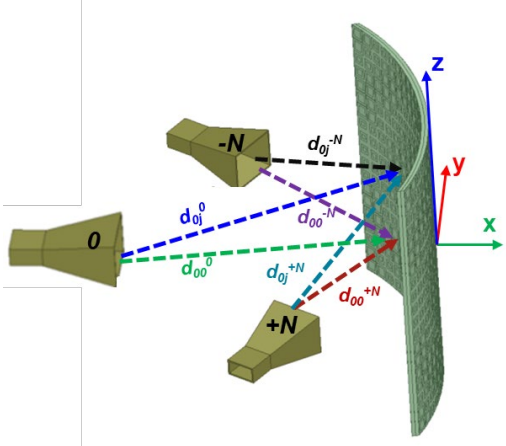

Fig. 11. Elliptical transmitarray for wide-angle beam scanning and multibeam radiation [69].

3) *Parallel Plate Antennas*

Conventional reflector antennas are not suited for base station antennas due to the difficulties of integrating them into the main base station antenna architecture. However, the parallel plate antenna, which consists of two plates and a field distribution mechanism in between, does serve as an attractive antenna candidate for mm-wave base stations. With a broad horizontal beam and narrow vertical beams, such an antenna could be used to replace the vertical linear arrays employed in current base stations. Its advantages include high efficiency and simplicity in the feed. The most common type of parallel plate antenna is the pillbox antenna [74], [75]. A pillbox antenna is a cylindrical reflector sandwiched between parallel plates, typically fed by a waveguide. By shaping the internal reflector, one can optimize the radiation pattern in elevation.

In [76], a multibeam leaky-wave pillbox antenna is reported. The antenna consists of three main components: integrated horns as the feeding part, a pillbox antenna, and the radiating part consisting of a printed leaky-wave antenna, namely an array of slots etched on the uppermost metal layer. The radiating and feeding parts are placed in two different stacked substrates connected by an optimized pillbox antenna. In contrast to conventional pillbox antennas, the quasi-optical system is made by a pin-made integrated parabola and several coupling slots optimized to efficiently transfer the energy from the feeding part to the radiating part. Seven pin-made integrated horns are placed in the focal plane of the integrated parabola to radiate seven beams in the far field. In [77], a differential feeding strategy is introduced to the leaky wave antenna to extend the operating bandwidth.

In [78], a fully metallic Luneburg lens based on the pillbox configuration operating in the Ka-band is reported. The parallel plate is loaded with glide-symmetric holes to produce the required equivalent refractive index profile of a Luneburg lens. Glide symmetry and inner metallic pins are employed to increase the equivalent refractive index. In [79], a broadband metasurface Luneburg lens is reported for full-angle operation. The design of the Luneburg lens is based on an inverted substrate parallel-plate-waveguide structure with nonuniform circular holes etched on the upper metallic plate. This structure allows significant simplification of the fabrication process as the effective refractive index profile can be realized by varying the hole diameters. By introducing tapered microstrip ports that are evenly distributed on the circumference of the Luneburg lens, full-angle operation of the lens is achieved.

In [80], a mm-wave wideband wide-angle multibeam metallic lens-loaded planar Cassegrain antenna with a compact three-layered parallel plate waveguide configuration is reported. A phase correction approach based on a convex metallic lens over the output of a conventional Cassegrain beamformer is employed to maximize the antenna gain and minimize the sidelobe levels over a ±60° wide angle, supporting 22 beams. Although not exactly in the shape of parallel plates, an innovative multibeam antenna based on a fully metallic Luneburg lens is reported in [81]. By virtue of transformation optics, the equivalent refractive index profile is realized by turning the parallel plates into curved shapes without introducing extra inserts to the middle. Eleven beams in an angular range of ±62.5° are obtained to operate from 25 and 36 GHz.

Not all the above configurations can be easily implemented as part of a high-frequency 6G base station antenna. However, the concepts will undoubtedly be an inspiration in our endeavors to 6G and beyond.

IV. Collocation of Multi-Band Antennas

One of the major challenges for the deployment of cellular networks is base station site acquisition. The process is not only expensive but also time-consuming. Therefore, it has become a common practice to collocate base station antennas to save antenna real estate. The objective is to integrate multiple antennas in a common limited space, allowing their operations across different frequency bands with minimal interference. This approach gained traction in the 2000s with the transition from 2G to 3G and the rollout of 4G. Currently, most base stations support multiple generations of systems employing collocated multi-band antennas occupying a shared aperture.

The advantages of collocating multiple antennas, such as reduced size and lower cost, are obvious, but this configuration also introduces strong electromagnetic interference between antennas. The interference can affect impedance matching,

reduce port isolation, and deteriorate the radiation patterns of all collocated antennas. Therefore, significant research efforts have been focused on minimizing the interference between antennas to enable efficient collocation [41]. One such technique is to employ metasurface cloaks [82], [83].

The interference effects between two antennas can be classified into two categories, namely, mutual coupling and scattering. Mutual coupling commonly refers to the interaction of two closely placed antennas operating in the same band. It tends to deteriorate the impedance matching performance and cause a change to the radiation pattern. This is the cause of the difference between the element pattern and the embedded or active element pattern in antenna arrays. If the two antennas operate in two different bands, one antenna will scatter the radiation from the other, thereby causing distortion of the radiation pattern. In the meantime, the impedance will also be changed due to the reflected currents induced by the scattering field.

To reduce the coupling and distortion in the radiation patterns, we can resort to decoupling and de-scattering techniques. Decoupling is a well-known issue for antenna arrays and numerous techniques have been developed to address it. The most used mutual coupling reduction techniques include electromagnetic band-gap (EBG) structures, defected ground structures (DGSs), neutralization lines, polarization rotators, decoupling surfaces, metamaterial structures, parasitic resonators, and filtering [4]. De-scattering is used primarily to reduce the effect of pattern distortion caused by the collocation of antennas operating in different bands, though it also improves impedance matching.

In comparison to antenna decoupling, antenna de-scattering only became an active research topic recently. The primary reason is that the main scattering effect, i.e., distortion of the radiation pattern by adjacent antenna elements at different bands, was not a significant issue in the nascent development of wireless systems due to simple frequency allocations. But now, most base station antennas contain collocated multiple antenna arrays for different frequency bands interleaved and/or side by side. Fig.12 illustrates a state-of-the-art base station antenna. The densely packed antenna panel as seen in Fig. 12 has been enabled by the continuous pursuit of antenna miniaturization and multi-functionalities, but it has also made it difficult to maintain element radiation patterns. Since early de-coupling techniques only aimed to reduce the transfer of power between the antenna elements, they typically contributed little to the mitigation of the radiation pattern distortion due to mutual scattering [84]. In theory, one could make the scatterers “invisible” by cloaking, but the problem is that most cloaking techniques are effective only within a limited bandwidth [85], [86], [87].

As seen in Fig. 12, base station antennas employ several linear arrays of dipole or patch elements to support MIMO. These antenna elements have significantly different sizes for different frequency bands from 800 MHz to 5 GHz. These arrays at different bands are interleaved side-by-side to save space. Naturally, larger antennas in lower bands would cause more distortion to the radiation patterns of smaller antennas at the higher band. Most recently, major de-scattering efforts have been made, and several new techniques have been developed to suppress cross-band scattering effectively. These de-scattering techniques include filtering, antenna topology optimization, cloaking and buffering.

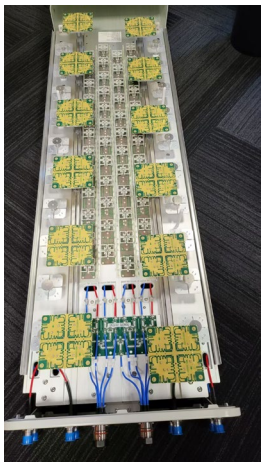

Fig. 12. A commercial tri-band base station antenna.

In [88], a method to suppress cross-band scattering in dual-band dual-polarized antenna arrays is first reported. The method involves introducing chokes into low-band (LB) elements to suppress high-band (HB) scattering currents induced on the LB elements. By inserting LB-pass HB-stop chokes into LB radiators, effective suppression of induced HB currents on the LB elements can be achieved. This greatly reduces the pattern distortion of the HB array caused by the presence of LB elements. The array considered is configured as two columns of HB antennas operating from 1.71 to 2.28 GHz interleaved with a single column of LB antennas operating from 0.82 to 1.0 GHz. The realized array with choked LB elements has stable and symmetrical beam patterns in both LB and HB. In [89], a systematic method to design an LB spatial-filtering antenna, which can efficiently suppress the blockage effect in the HB and maintain LB antenna performance is reported. The LB antenna achieved a 0.69–0.96 bandwidth.

Built on the success in [88], a distributed choking technique, the spiral choke, for scattering suppression in dual-band dual-polarization antenna arrays is reported [90] to improve de-scattering bandwidth. The spiral chokes are implemented as low-band radiators in collocated 4G and 5G dual-band arrays to suppress cross-band scattering while broadening the bandwidth of the choked element. The experimental results demonstrate that the cross-band scattering in the array is largely eliminated, and the realized dual-band array has very stable radiation performance in both well-matched bands.

The detrimental effect of HB elements on LB radiation performance is first analyzed in [91], and a capacitance-loaded HB element is introduced to restore the LB beam patterns. Further, to eliminate the reverse HB scattering caused by the LB element while enhancing the bandwidth of the LB element, a novel double-arm choked cross-dipole configuration is proposed. The experimental results of the array show a largely suppressed cross-band scattering with stable radiation performance across the well-matched bands.

In [92], a filtered bowl-shaped LB antenna covering 0.80–0.96 GHz for dual-band base station antenna arrays is introduced to reduce its effect on the HB antenna, as shown in Fig. 13. By incorporating helical filters into the LB radiators, a

significant de-scattering HB bandwidth reaching 66.7% (1.36–2.72 GHz) is achieved. To improve the LB impedance bandwidth, specialized LC circuits are incorporated into the LB balun. These LC circuits, in conjunction with the baffles, serve to ease the gain fluctuations of the HB antenna placed inside the LB antenna. In addition, the miniaturized aperture size of the LB antenna enhances in-band isolation in the array. In [93], a broadband dual-polarized electromagnetic transparent antenna is introduced. De-scattering is achieved by etching nested split-slot resonators (N-SSRs) on the entire radiating arms. These N-SSRs can form two independently controllable de-scattering bands.

Fig. 13. A bow-shaped LB antenna with an embedded HB antenna in it [92].

The more bands that are employed, the more difficult it becomes to perform effective de-scattering. Most recently, a quadruple-band shared aperture (QBSA) antenna array was reported in [94]. The QBSA array consists of a LB antenna (0.78–1.08 GHz), two groups of middle-band (MB) antennas (1.7–2.1 GHz), and a HB array covering two individual bands including 3.4–3.6 GHz and 4.7–4.9 GHz, all arranged in an interleaved configuration. To maintain normal radiation patterns, the radiating patches of the LB antenna were converted into electromagnetically transparent structures. This was accomplished by incorporating corresponding multi-FSS structures designed to operate within the frequency bands of the MB and HB antennas. The MB antenna also incorporates dual-band Jerusalem slots within its radiating patches to ameliorate the blockage effect.

A new de-scattering method called buffering was developed recently for a shared-aperture dual-band array [95]. The developed array covers 0.69-0.96 GHz (32.7%) in the LB and 1.47-2.7 GHz (59.0%) in the HB. Offering a compact size with an exceptionally low profile, see Fig. 14. Unlike the previous schemes that focused on LB-HB isolation, this buffering-scheme-based array introduced a unique tightly-coupled buffering layer (TCBL) that serves as a buffer and is tightly coupled with both LB and HB radiators. It plays two crucial roles: in the LB, the TCBL functions as a reactance-compensation loading that enables a significantly low profile of the LB antenna. This leads to a reduced blockage effect on surrounding HB antennas, thus ensuring unobstructed HB radiation. In the HB, the TCBL enables a new resonant mode, expanding the HB bandwidth from 45.5% to 59.0%. Meanwhile, the array effectuates effective cross-band isolation without introducing extra filtering designs, as the TCBL prevents the electromagnetic energy from transferring to the cross-band ports.

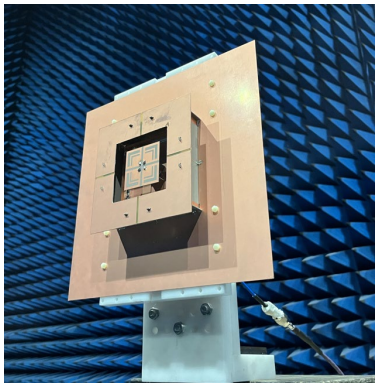

Fig. 14. A de-scattered antenna employing a buffering scheme [95].

V. Antenna Designs Employing AI

Given the increased complexity of 6G antennas and the rapidly increasing AI capabilities being developed, it is expected that AI will play a key role in 6G antenna system designs. Traditionally, antennas were designed using EM simulation software, such as HFSS and Microwave CST, where the dimensions were iteratively adjusted through trial-and-error. This approach is time-consuming, as it necessitates numerous EM simulations. Furthermore, the vast number of possible parameter combinations makes it challenging to efficiently achieve optimal designs. To address these challenges, numerous machine learning (ML) techniques have been introduced as data-driven surrogate models, offering an alternative to EM simulations in antenna designs. Well-trained ML models can predict antenna behavior and deliver automatic designs. More importantly, as AI will be an integral part of 6G, it is envisaged that it will facilitate the in-situ reconfiguration of 6G antenna systems in order to realize optimal system performance for any given radio environment. In the following, we aim to review the most recent studies on the application of AI to antenna designs, array synthesis and metasurfaces.

A. AI-based Antenna Element Design

Among the studies on ML-based antenna designs, many focus on developing surrogate models that utilize ML methods to efficiently predict antenna performance. These studies typically involve training a model using EM-simulated datasets, where the antenna parameters serve as inputs, and antenna performance metrics, such as bandwidth and gain, are treated as outputs. The primary goal is to achieve accurate predictions of antenna characteristics in a significantly shorter time compared to traditional EM simulators. For example, a convolutional neural network (CNN) is presented in [96] to predict the resonant frequencies of a dual-band pixelated microstrip antenna. Based on the base structure of the pixelated microstrip antenna, the CNN model is trained to predict its resonant frequencies. In [97], a novel pyramidal deep regression network (PDRN) is introduced to accurately predict the frequency responses of antennas. The PDRN features a pyramidal-like structure of neural networks, with its hyperparameters determined through Bayesian optimization.

Many studies have also focused on the optimization of antenna performance using surrogate models. Stochastic algorithms are typically utilized in conjunction with ML models to achieve these optimizations. For instance, a

backpropagation-multilayer perceptron (MLP) neural network (BPNN) is developed as a surrogate model, and a multi-objective Genetic Algorithm (GA) is used to optimize antenna performance in [98]. Other work in the field addressed multi-objective modelling and optimizations for antenna designs [99]. An arguably more interesting application of AI to antenna designs is to take desired antenna performance as the input and optimal geometrical parameters as the output. To this end, an inverse artificial neural network (ANN) model for convenient multi-objective antenna design is presented in [100]. The model addresses the multi-objective challenge of antenna designs through a two-part structure: the first component consists of three parallel and independent branches dedicated to S-parameters, the gain, and radiation pattern, while the second component provides the final predicted results. Once trained, the inverse model can directly generate antenna geometries without needing iterative calls from an optimization algorithm.

B. AI-based Array Synthesis

Many ML-powered methods have been proposed to deal with different array synthesis problems. In comparison to traditional approaches that generally required many iterations of optimization, ML-based methods can significantly expedite the design process, making real-time array synthesis possible. Additionally, some models are able to accurately predict complex mutual coupling conditions for nonuniform array antennas.

Excitation phase optimization of an array for desired radiation power patterns is an important topic in array synthesis, particularly for metasurface or reflectarray/transmitarray design. In [101], a radial basis function neural network (RBFNN) with a Gaussian activation function is reported for phase-only nulling with low sidelobe levels. The RBFNN structure, including the number of neurons in the hidden layer, is optimized with a self-adaptive differential evolution (SADE) for optimal performance. It is trained with the beam direction and null direction as input and excitation phases as output.

Several studies have also been reported to employ ML-based methods to optimize the excitation amplitudes of antenna arrays. In [102], a generalized regression neural network (GRNN) is introduced for synthesizing low-sidelobe scanning beam patterns in conformal arrays. The GRNN can output excitation amplitudes based on inputs including beam directions and sidelobe levels. Some other studies have been conducted for the synthesis of non-uniform or sparse arrays. These methods focus on optimizing the array distribution with/without excitation modulation for desired array radiation patterns. In [103], a novel multibranch encoder-decoder-based ANN framework is developed for pattern-reconfigurable nonuniformly spaced linear array synthesis. In the framework, multiple encoder–decoder branches are devoted to synthesizing multiple different radiation patterns. By minimizing a loss function with respect to multiple radiation patterns, element amplitudes and positions with minimum inter-element spacing control can be obtained.

Given the dynamic nature of mobile communications networks, it is expected that reinforcement learning will serve as a critical technique to enhance the intelligence of future antenna systems, making the antennas cognitive [51]. Such antennas will be able to adapt their radiation patterns and operating bandwidth according to the radio and system requirements. To this end, [104] introduced deep reinforcement learning (DRL) to adaptive multibeam steering employing the generalized joined coupler (GJC) matrix as a dynamic feed network. By learning the user movement and therefore the required beam directions, the DRL algorithm provides in-situ control of the phase shifters to steer different beams in different directions.

C. AI-based Metasurface Design

Conventionally, the design of metasurface unit cells relies on optimization loops of time-consuming and resource-demanding full-wave simulations. While experience can expedite the design process, adequate exploration of the design space remains challenging. Recently, several ML methods have been employed in metasurface designs to accurately predict the scattering properties of metasurface unit cells based on their physical parameters. For example, in [105], an ANN-based modified multilayer perceptron (M2LP) is proposed for reflectarray design. The architecture of the M2LP is optimized by using the Bayesian Optimization algorithm.

In contrast to forward prediction, the inverse design of unit cell structures and dimensions based on desired properties is more challenging. This difficulty arises from the one-to-many nature of the mapping, where a single set of desired scattering properties can correspond to multiple possible unit cell dimensions. A number of ML methods have been presented for the inverse design of metasurfaces. To address the non-uniqueness problem, for example, an improved transfer function (TF)-based ANN model is developed in [106].

In [107], a deep learning framework, named Deep UCGAN++, is developed to streamline and enhance the design of hybrid-functional metasurfaces. By leveraging a deep Unet++ generative adversarial network (GAN) architecture, the proposed model enables accurate forward prediction of EM responses and inverse design capabilities based on user-defined functionalities. The model's hybrid-mode database allows for flexible, freeform pattern generation, addressing the limitations in design freedom and model generalization.

Some ML methods have been presented for the design of multi-layer metasurfaces. Given their increased degrees of freedom, multi-layer metasurfaces offer both significant potential and substantial optimization challenges. Typically, the design space for a multi-layer metasurface encompasses various scatterer shapes, resulting in a high-dimensional space that makes it challenging to find the global optimum. In [108], a prior-knowledge-guided deep-learning-enabled (PK-DL) synthesis method is introduced, specifically using a conditional deep convolutional GAN (cDCGAN), for the design of metalens antennas.

In [109], a generative ML-based approach is presented to automate the inverse design of dual- and triple-layer metasurfaces. Specifically, using a generative ML model based on a variational autoencoder (VAE), the structures and the scattering properties of the multilayer metasurfaces in the training set are converted into a low-dimensional continuous latent space. In this latent space, the particle swarm optimization (PSO) algorithm is performed to find the optimum latent variables.

VI. Concluding Remarks

As outlined above, new 6G features and functionalities pose both challenges and opportunities for antenna research and engineering. To conclude the paper, we would like to share the following thoughts to catalyse future 6G antenna research.

First, the integration of terrestrial and non-terrestrial networks demands antenna innovation not only for new platforms, such as LEO satellites, UAVs and HAPS, but also for the seamless integration of the two networks and services. For example, the design of future base station antennas needs to consider both the support of UAVs and the interference to aircrafts. Such requirements serve as a paradigm shift from current ones.

Second, although 6G systems have yet to be standardized, the introduction of new frequency bands and technologies is anticipated, bringing both significant challenges and opportunities for multiband collocated antenna arrays. 6G is expected to introduce a new mid-band frequency range from 7 to 15 GHz, including distinct bands such as 7.125–8.5 GHz, 10.7–13.25 GHz, and 14–15.35 GHz [38], [39]. Considering that current shared-aperture antennas already have difficulties supporting various frequency bands for 4G and 5G, new innovations are needed to integrate 4G, 5G, and 6G bands within a single shared-aperture. For high frequency including mm-wave systems, lens and parallel plate antennas may play a major role in reducing the complexity and losses of feed networks.

Third, high-gain multibeam and wide-angle scanning capabilities will be important for 6G systems to support ISAC, airborne and spaceborne systems, applications such as enhanced sidelink communications, network reliability and throughput, and efficient use of radio resources. These antennas need to be low-cost and consume minimal energy. These are very challenging tasks. For instance, there is an inherent contradiction between achieving a wide radiation pattern for individual elements and maintaining low coupling—both of which are critical for wide-angle beamforming [110].

Finally, the application of AI to the field of antennas is still in its infancy, so there are still numerous challenges to be addressed. While the trained model may facilitate real-time antenna designs, obtaining the training dataset is typically laborious and time-consuming. Consequently, current ML-based antenna design studies typically only focus on the design or optimization of a limited number of parameters. New research is needed to ease this limitation to accommodate massive antenna arrays and reconfigurable intelligent surfaces. Furthermore, whilst the ML models generated for specific antenna designs may perform well, they often fail to adapt to other antenna structures or design constraints. In fact, the antenna design should be part of the overall transceiver optimization process in a digital twin. It is a challenge to create ML models that work for a broad range of systems. Most importantly, 6G antennas would need to operate autonomously with the AI-innate 6G networks. Therefore, it is important to develop new antenna architectures and ML models that work hand-in-hand to achieve the goal of autonomous networks with minimal energy consumption [111].

References

[1] T. Gong et al., "Holographic MIMO communications: Theoretical foundations, enabling technologies, and future directions," *IEEE Commun. Surv. Tutor.*, vol. 26, no. 1, pp. 196-257, 2024.

[2] W. Chen et al., "5G-advanced toward 6G: Past, present, and future," *IEEE J. Sel. Areas Commun.*, vol. 41, no. 6, pp. 1592-1619, Jun. 2023.

[3] You, X., Wang, CX., Huang, J. *et al.* Towards 6G wireless communication networks: vision, enabling technologies, and new paradigm shifts. *Sci. China Inf. Sci.* **64**, 110301 (2021).

[4] Y. J. Guo and R. W. Ziolkowski, *Advanced Antenna Array Engineering for 6G and Beyond Wireless Communications*, Hoboken, NJ, USA: Wiley, 2021.

[5] International Telecommunication Union, "Framework and overall objectiv es of the future development of IMT for 2030 and beyond," Recommendation ITU-R M.2160-0, Nov. 2023. https://www.itu.int/dms_pubrec/itu-r/rec/m/R-REC-M.2160-0-202311-I%21%21PDF-E.pdf

[6] S. Lu *et al*., "Integrated sensing and communications: Recent advances and ten open challenges," in *IEEE Internet Things J.*, vol. 11, no. 11, pp. 19094-19120, Jun. 2024.

[7] K. Wu, J. A. Zhang, and Y. J. Guo, *Joint Communications and Sensing: From Fundamentals to Advanced Techniques. Hoboken*, NJ, USA: Wiley, 2022.

[8] K. Wu, J. A. Zhang, X. Huang, R. W. Heath, and Y. J. Guo, "Green joint communications and sensing employing analog multi-beam antenna arrays," *IEEE Commun. Mag.*, vol. 61, no. 7, pp. 172-178, Jul. 2023.

[9] R. Shrivastava, S. Hegde, and O. Blume, "Sidelink evolution toward 5G-A/6G future considerations for standardization of group communications," *IEEE Commun. Standards Mag.*, vol. 7, no. 1, pp. 24-30, Mar. 2023.

[10] J. Wigard *et al*., "Ubiquitous 6G service through non-terrestrial networks," *IEEE Wireless Commun.*, vol. 30, no. 6, pp. 12-18, Dec. 2023.

[11] M. M. Saad, M. A. Tariq, M. T. R. Khan, and D. Kim, "Non-terrestrial networks: An overview of 3GPP release 17 & 18," *IEEE Internet Things Mag.*, vol. 7, no. 1, pp. 20-26, Jan. 2024.

[12] J. G. Hernández, C. C. Martín, and N. Talayero, "Direct-to-device satellite service: a complement to mobile networks," Telefónica. Accessed: Feb. 18, 2025. [Online] Available: https://www.telefonica.com/en/communication-room/blog/direct-device-satellite-service-complement-mobile-networks/.

[13] "Technologies & Standards to Enable Vertical Ecosystem Transformation in 6G." Network World Europe. [Online] Available: https://bscw.sns-ju.eu/pub/bscw.cgi/d95695/White%20Paper1_WG_Enabling_Technologies_final.pdf.

[14] W. Roh *et al.*, "Millimeter-wave beamforming as an enabling technology for 5G cellular communications: Theoretical feasibility and prototype results," *IEEE Commun. Mag.*, vol. 52, no. 2, pp. 106–113, Feb. 2014.

[15] R. W. Heath Jr., N. González-Prelcic, S. Rangan, W. Roh, and A. M. Sayeed, "An overview of signal processing techniques for millimeter wave MIMO systems," *IEEE J. Sel. Topics Signal Process.*, vol. 10, no. 3, pp. 436-453, Apr. 2016.

[16] Y. J. Guo, J. Bunton, V. Dyadyuk, and X. Huang, "Hybrid adaptive antenna array," U.S. Patent US8754810, Jun. 2014.

[17] X. Huang, Y. J. Guo, and J. Bunton, "A hybrid adaptive antenna array", *IEEE Trans. Wireless Commun.,* vol. 9, no. 5, pp. 1770-1779, May 2010.

[18] Y. J. Guo and B. Jones, "Base station antennas," in *Antenna Engineering Handbook*, 4th ed. New York, NY, USA: McGraw-Hill, 2007.

[19] Y. J. Guo, M. Ansari, R. W. Ziolkowski, and N. J. G. Fonseca, "Quasi-optical multi-beam antenna technologies for B5G and 6G mmWave and THz networks: A review," *IEEE Open J. Antennas Propag.*, vol. 2, pp. 807-830, 2021.

[20] Y. J. Guo, M. Ansari, and N. J. G. Fonseca, "Circuit type multiple beamforming networks for antenna arrays in 5G and 6G terrestrial and non-terrestrial networks," *IEEE J. Microw.*, vol. 1, no. 3, pp. 704-722, Jul. 2021.

[21] C. A. Guo and Y. J. Guo, "A general approach for synthesizing multibeam antenna arrays employing generalized joined coupler matrix," *IEEE Trans. Antennas Propag.*, vol. 70, no. 9, pp. 7556-7564, Sep. 2022.

[22] C. L. Holloway, E. F. Kuester, J. A. Gordon, J. O'Hara, J. Booth, and D. R. Smith, "An overview of the theory and applications of metasurfaces: The two-dimensional equivalents of metamaterials," *IEEE Antennas Propag. Mag.*, vol. 54, no. 2, pp. 10-35, Apr. 2012.

[23] S. S. Bukhari, J. Vardaxoglou, and W. Whittow, "A metasurfaces review: Definitions and applications," *Appl. Sci*., vol. 9, no. 13, p. 2727, Jul. 2019.

[24] N. Shlezinger, G. C. Alexandropoulos, M. F. Imani, Y. C. Eldar, and D. R. Smith, "Dynamic metasurface antennas for 6G extreme massive MIMO communications," *IEEE Wireless Commun.*, vol. 28, no. 2, pp. 106-113, Apr. 2021.

[25] T. A. Tsiftsis, C. Valagiannopoulos, H. Liu, A.-A. A. Boulogeorgos, and N. I. Miridakis, "Metasurface-coated devices: A new paradigm for energy-

efficient and secure 6G communications," *IEEE Veh. Technol. Mag.*, vol. 17, no. 1, pp. 27–36, Mar. 2022.
[26] M. D. Renzo et al., "Smart radio environments empowered by reconfigurable intelligent surfaces: How it works, state of research, and the road ahead," *IEEE J. Sel. Areas Commun.*, vol. 38, no. 11, pp. 2450-2525, Nov. 2020.
[27] V. G. Ataloglou et al., "Static and reconfigurable Huygens' metasurfaces: Use in antenna beamforming and beam steering," *IEEE Antennas Propag. Mag.,* vol. 64, no. 4, pp. 73-84, Aug. 2022.
[28] L. Qi, S. Gao, X. X. Yang and J. T. S. Sumantyo, Ch. 3, "Low-Cost Beam-Reconfigurable Directional Antennas for Advanced Communications,", in Y. J. Guo and R. W. Ziolkowski, *Antenna and Array Technologies for Future Wireless Ecosystems*, Hoboken, NJ, USA: Wiley, Aug. 2022.
[29] Y. J. Guo, P.-Y. Qin, S.-L. Chen, W. Lin, and R. W. Ziolkowski, "Advances in reconfigurable antenna systems facilitated by innovative technologies," *IEEE Access*, vol. 6, pp. 5780-5794, 2018.
[30] J. O. Martínez, J. R. Rodríguez, Y. Shen, K. -F. Tong, K. -K. Wong, and A. G. Armada, "Toward liquid reconfigurable antenna arrays for wireless communications," *IEEE Commun. Mag.*, vol. 60, no. 12, pp. 145-151, Dec. 2022.
[31] F. Zeng, C. Ding, and Y. J. Guo, "A reconfigurable millimeter-wave antenna array with wide-range continuous beamwidth control (WCBC) based on polarization-mixing," *IEEE Trans. Antennas Propag.*, vol. 72, no. 4, pp. 3092-3103, Apr. 2024.
[32] Y. He, G. Wei, R. W. Ziolkowski, and Y. J. Guo, "An ultrawideband frequency-reconfigurable tightly coupled dipole array with wide beam-scanning capability," *IEEE Trans. Antennas Propag.*, vol. 72, no. 11, pp. 8488-8500, Nov. 2024.
[33] L. Zhu, W. Ma, and R. Zhang, "Movable antennas for wireless communication: Opportunities and challenges," *IEEE Commun. Mag.*, vol. 62, no. 6, pp. 114-120, Jun. 2024.
[34] A. Yadav, G. I. Tsiropoulos, and O. A. Dobre, "Full-duplex communications: Performance in ultradense mm-wave small-cell wireless networks," *IEEE Veh. Technol. Mag.*, vol. 13, no. 2, pp. 40-47, Jun. 2018.
[35] M. A. Elmansouri, A. J. Kee, and D. S. Filipovic, "Wideband antenna array for simultaneous transmit and receive (STAR) applications," *IEEE Antennas Wireless Propag. Lett.*, vol. 16, pp. 1277-1280, 2017.
[36] A. Tuyen Le, X. Huang, C. Ding, H. Zhang, and Y. J. Guo, "An in-band full-duplex prototype with joint self-interference cancellation in antenna, analog, and digital domains," *IEEE Trans. Microw. Theory Technol.*, vol. 72, no. 9, pp. 5540-5549, Sep. 2024.
[37] Y. Chen, C. Ding, Y. Jia, and Y. Liu, "Antenna/propagation domain self-interference cancellation (SIC) for in-band full-duplex wireless communication systems," *Sensors*, vol. 22, no. 5, pp. 1–18, 2022.
[38] "Spectrum for 6G explained." Nokia.com. Accessed: Nov. 13, 2024. [Online] Available: https://www.nokia.com/about-us/newsroom/articles/spectrum-for-6G-explained/.
[39] "6G Spectrum: Unleashing Extreme Performance." Ericsson.com. Accessed: Nov. 13, 2024. [Online] Available: https://www.ericsson.com/en/6g/spectrum.
[40] M. Monemi, S. Bahrami, M. Rasti, and M. Latva-aho, "A study on characterization of near-field sub-regions for phased-array antennas," *IEEE Trans. Commun*., early access, Oct. 2024, doi: 10.1109/TCOMM.2024.3483046.
[41] J. An, C. Yuen, L. Dai, M. Di Renzo, M. Debbah, and L. Hanzo, "Near-field communications: Research advances, potential, and challenges," *IEEE Wireless Commun*., vol. 31, no. 3, pp. 100-107, Jun. 2024.
[42] A. Ashyap, R. Raad, F. Tubbal, W. Ali Khan, and S. Abulgasem, "Highly bendable AMC-based antenna for wearable applications," *IEEE Access*, vol. 12, pp. 154195-154211, 2024.
[43] W. Zhu, X. Liu, Y. Fan, Z. Zhang, and X. Ma, "Transparent and flexible antenna with polarization reconfigurability using EGaIn for wearable applications," *IEEE Trans. Antennas Propag.*, vol. 72, no. 10, pp. 7493-7503, Oct. 2024.
[44] A. Kiran and G. K. Mishra, "Bluetooth, Wi-Fi, and Wi-Max supporting spectacles antenna for internet of things applications," *IEEE Internet Things J.*, vol. 11, no. 21, pp. 35185-35192, Nov. 2024.
[45] F. Pervez, J. Qadir, M. Khalil, T. Yaqoob, U. Ashraf, and S. Younis, "Wireless technologies for emergency response: A comprehensive review and some guidelines," *IEEE Access*, vol. 6, pp. 71814-71838, 2018.
[46] J. Butler and R. Lowe, "Beam-forming matrix simplifies design of electronically scanned antennas," *Electron. Des.*, pp. 170–173, Apr. 1961.
[47] J. Blass, "Multidirectionnal antenna, a new approach to stacked beams," *IRE Int. Conf. Record*, vol. 8, pt. 1, pp. 48–50, 1960.
[48] S. Mosca et al., "A novel design method for Blass matrix beam-forming networks," *IEEE Trans. Antennas Propag.*, vol. 50, no. 2, pp. 225–232, Feb. 2002.
[49] C. A. Guo, Y. J. Guo, H. Zhu, W. Ni, and J. Yuan, "Optimization of multibeam antennas employing generalized joined coupler matrix," *IEEE Trans. Antennas Propag.*, vol. 71, no. 1, pp. 215-224, Jan. 2023.
[50] C. A. Guo, Y. J. Guo, and J. Yuan, "Multibeam receiving antennas employing generalized joined coupler matrix," *IEEE Trans. Antennas Propag.*, vol. 72, no. 1, pp. 424-432, Jan. 2024.
[51] J. Nolen, "Synthesis of multiple beam networks for arbitrary illuminations," *Ph.D. dissertation*, *Radio Div*., *Bendix Corp*., *Baltimore*, *MD*, USA, 1965.
[52] N. J. G. Fonseca, "Printed S-band 4 × 4 Nolen matrix for multiple beam antenna applications," *IEEE Trans. Antennas Propag.*, vol. 57, no. 6, pp. 1673-1678, Jun. 2009.
[53] T. Djerafi, N. J. G. Fonseca, and K. Wu, "Broadband substrate integrated waveguide 4×4 Nolen matrix based on coupler delay compensation," *IEEE Trans. Microw. Theory Technol.*, vol. 59, no. 7, pp. 1740-1745, Jul. 2011.
[54] H. Zhu, T. Zhang, and Y. J. Guo, "Wideband hybrid couplers with unequal power division/arbitrary output phases and applications to miniaturized Nolen matrices," *IEEE Trans. Microw. Theory Technol.*, vol. 70, no. 6, pp. 3040-3053, Jun. 2022.
[55] Y. Yang, Y. F. Pan, S. Y. Zheng, W. Hong, and W. S. Chan, "Analytical design method and implementation of broadband 4 × 4 Nolen matrix," *IEEE Trans. Microw. Theory Technol.*, vol. 70, no. 1, pp. 343-355, Jan. 2022.
[56] Y. Xu, H. Zhu, and Y. J. Guo, "Compact wideband 3 × 3 Nolen matrix with couplers integrated with phase shifters," *IEEE Microw. Wireless Technol. Lett.*, vol. 34, no. 2, pp. 159-162, Feb. 2024.
[57] H. Liu, X. Gu, and H. Tian, "Design of extended Nolen matrix with enhanced beam controllability and widened spatial coverage," *IEEE Trans. Circuits and Syst. II: Express Briefs*, vol. 71, no. 7, pp. 3273-3277, Jul. 2024.
[58] K. Wu and Y. J. Guo, "Deterministic solutions to improved generalized joined coupler matrix for multibeam antennas," *IEEE Trans. Antennas Propag.*, vol. 71, no. 12, pp. 9454-9466, Dec. 2023.
[59] M. A. Fuentes-Pascual, M. Ferrando-Rocher, J. I. Herranz-Herruzo, and M. Baquero-Escudero, "Five-beam fully metallic Nolen matrix-based array antenna for 5G applications at 26 GHz," *IEEE Trans. Antennas Propag.*, vol. 72, no. 11, pp. 8852-8857, Nov. 2024.
[60] H. Ren, H. Zhang, Y. Jin, Y. Gu, and B. Arigong, "A novel 2-D 3×3 Nolen matrix for 2-D beamforming applications," *IEEE Trans. Microw. Theory Technol.*, vol. 67, no. 11, pp. 4622-4631, Nov. 2019.
[61] Y. Yang, Y. F. Pan, W. S. Chan, and S. Y. Zheng, "Dimension expansion method and implementation of broadband planar 2-D 3 × 3 Nolen matrix," *IEEE Trans. Antennas Propag.*, vol. 71, no. 9, pp. 7395-7408, Sep. 2023.
[62] M. Ansari, B. Jones, H. Zhu, N. Shariati, and Y. J. Guo, "A highly efficient spherical Luneburg lens for low microwave frequencies realized with a metal-based artificial medium," *IEEE Trans. Antennas Propag.*, vol. 69, no. 7, pp. 3758-3770, Jul. 2021.
[63] J.-W. Lian, M. Ansari, P. Hu, Y. J. Guo, and D. Ding, "Wideband and high-efficiency parallel-plate Luneburg lens employing all-metal metamaterial for multibeam antenna applications," *IEEE Trans. Antennas Propag.*, vol. 71, no. 4, pp. 3193-3203, Apr. 2023.
[64] S. Lei, G. Wei, K. Han, X. Li, and T. Qiu, "A wideband 3-D-printed multibeam circularly polarized ultrathin dielectric slab waveguide Luneburg lens antenna," *IEEE Antennas Wireless Propag. Lett.*, vol. 21, no. 8, pp. 1582-1586, Aug. 2022.
[65] C. Bilitos, X. Morvan, R. Sauleau, E. Martini, S. Maci, and D. González-Ovejero, "Series dual-fed continuous transverse stub array with enhanced multibeam operation enabled by a reflective Luneburg lens," *IEEE Trans. Antennas Propag.*, vol. 72, no. 11, pp. 8420-8432, Nov. 2024.
[66] F. Meng, Y. Guo, K. Ma, and Y. Luo, "A Terahertz wide-angle beamsteering 3-D printed half-compressed elliptical Luneburg lens with planar focal plane," *IEEE Antennas Wireless Propag. Lett.*, vol. 23, no. 2, pp. 843-847, Feb. 2024.
[67] F. Maggiorelli, A. Paraskevopoulos, J. Vardaxoglou, M. Albani, and S. Mci, "Notes on profile inversion and closed form formulation of compact GRIN lenses," *IEEE Open J. Antennas Propag.*, vol. 2, pp. 976-977, 2021.
[68] L.-Z. Song, M. Ansari, P.-Y. Qin, S. Maci, J. Du, and Y. J. Guo, "Two-dimensional wide-angle multibeam flat GRIN lens with a high aperture efficiency," *IEEE Trans. Antennas Propag.*, vol. 71, no. 10, pp. 8018-8029, Oct. 2023.
[69] L.-Z. Song, P.-Y. Qin, S.-L. Chen, and Y. J. Guo, "An elliptical cylindrical shaped transmitarray for wide-angle multibeam applications," *IEEE Trans. Antennas Propag.*, vol. 69, no. 10, pp. 7023-7028, Oct. 2021.

[70] T. Chen, L. Song, and Y. Liu, "A broadband dual-polarized reconfigurable transmitarray with sum and difference beam-steering capabilities," *IEEE Trans. Antennas Propag.*, vol. 72, no. 10, pp. 8052-8057, Oct. 2024.
[71] X. Wang, P.-Y. Qin, A. Tuyen Le, H. Zhang, R. Jin, and Y. J. Guo, "Beam scanning transmitarray employing reconfigurable dual-layer Huygens element," *IEEE Trans. Antennas Propag.*, vol. 70, no. 9, pp. 7491-7500, Sep. 2022.
[72] X. He, W. Yang, Y. Li, Q. Xue, and W. Che, "W-band wideband transmit-array antenna based on multiresonance multimode Huygens metasurface," *IEEE Trans. Antennas Propag.*, vol. 72, no. 9, pp. 7299-7304, Sep. 2024.
[73] J.-W. Lian, Y.-L. Ban, and Y. J. Guo, "Wideband dual-layer Huygens' metasurface for high-gain multibeam array antennas," *IEEE Trans. Antennas Propag.*, vol. 69, no. 11, pp. 7521-7531, Nov. 2021.
[74] W. Rotman, "Wide-angle scanning with microwave double-layer pillboxes," *IRE Trans. Antennas Propag.*, vol. 6, no. 1, pp. 96-105, Jan. 1958.
[75] E. L. Holzman, "Pillbox antenna design for millimeter-wave base-station applications," *IEEE Antennas Propag. Mag.*, vol. 45, no. 1, pp. 27-37, Feb. 2003.
[76] M. Ettorre, R. Sauleau, and L. Le Coq, "Multi-beam multi-layer leaky-wave SIW pillbox antenna for millimeter-wave applications," *IEEE Trans. Antennas Propag.*, vol. 59, no. 4, pp. 1093-1100, Apr. 2011.
[77] Y. Cao, S. Yan, W. Liu, and J. Li, "A wideband multibeam pillbox antenna based on differentially fed leaky-wave array," *IEEE Antennas Wireless Propag. Lett.*, vol. 22, no. 3, pp. 512-516, Mar. 2023.
[78] O. Quevedo-Teruel, J. Miao, M. Mattsson, A. Algaba-Brazalez, M. Johansson, and L. Manholm, "Glide-symmetric fully metallic Luneburg lens for 5G communications at Ka-band," *IEEE Antennas Wireless Propag. Lett.*, vol. 17, no. 9, pp. 1588-1592, Sep. 2018.
[79] J. Li *et al*., "Design of a broadband metasurface Luneburg lens for full-angle operation," *IEEE Trans. Antennas Propag.*, vol. 67, no. 4, pp. 2442-2451, Apr. 2019.
[80] Y. Bi, Y. Li, M. Chen, J. Wang, L. Ge, and J. Li, "A millimeter-wave phase correction metallic lens loaded planar Cassegrain antenna with wide-angle multibeam radiation," *IEEE Trans. Antennas Propag.*, vol. 72, no. 8, pp. 6753-6758, Aug. 2024.
[81] Q. Liao, N. J. G. Fonseca, and O. Quevedo-Teruel, "Compact multibeam fully metallic geodesic Luneburg lens antenna based on non-Euclidean transformation optics," *IEEE Trans. Antennas Propag.*, vol. 66, no. 12, pp. 7383-7388, Dec. 2018.
[82] A. Monti et al., "Mantle cloaking for co-site radio-frequency antennas," *Appl. Phys. Lett*., vol. 108, no. 11, Mar. 2016, Art. no. 113502.
[83] J. Soric, Y. Ra'di, D. Farfan, and A. Alù, "Radio-transparent dipole antenna based on a metasurface cloak," *Nature Commun*., vol. 13, no. 1, p. 1114, Mar. 2022.
[84] Y. Zhang, X. Y. Zhang, L. Ye, and Y. Pan, "Dual-band base station array using filtering antenna elements for mutual coupling suppression," *IEEE Trans. Antennas Propag.*, vol. 64, no. 8, pp. 3423-3430, Aug. 2016.
[85] M. Selvanayagam and G. V. Eleftheriades, "Experimental demonstration of active electromagnetic cloaking," *Phys. Rev. X*, vol. 3, no. 4, 041011, Nov. 2013.
[86] A. Alù, "Mantle cloak: Invisibility induced by a surface," *Phys. Rev. B*, vol. 80, no. 24, 245115, Dec. 2009.
[87] P. Chen, F. Monticone and A. Alù, "Suppressing the electromagnetic scattering with an helical mantle cloak," *IEEE Antennas Wireless Propag. Lett.*, vol. 10, pp. 1598-1601, 2011.
[88] H.-H. Sun, C. Ding, H. Zhu, and Y. J. Guo, "Suppression of cross-band scattering in multiband antenna arrays," *IEEE Trans. Antennas Propag.*, vol. 67, no. 4, pp. 2379-2389, Apr. 2019.
[89] Y. Wang, H. Su, R. C. Dai, L. T. Chen, L. H. Ye, and X. Y. Zhang, "A systematic approach to design spatial filtenna for aperture-shared base-station srray," *IEEE Trans. Antennas Propag.*, vol. 71, no. 10, pp. 7792-7803, Oct. 2023.
[90] H.-H. Sun, H. Zhu, C. Ding, B. Jones, and Y. J. Guo, "Scattering suppression in a 4G and 5G base station antenna array using spiral chokes," *IEEE Antennas Wireless Propag. Lett.*, vol. 19, no. 10, pp. 1818-1822, Oct. 2020.
[91] S.-Y. Sun, C. Ding, W. Jiang, and Y. J. Guo, "Simultaneous suppression of cross-band scattering and coupling between closely spaced dual-band dual-polarized antennas," *IEEE Trans. Antennas Propag.*, vol. 71, no. 8, pp. 6423-6434, Aug. 2023.
[92] Y. He, C. Ding, C. Chang, G. Wei, and Y. J. Guo, "A bowl-shaped filtering antenna with wideband cross-band scattering mitigation for dual-band base stations," *IEEE Trans. Antennas Propag.*, vol. 72, no. 8, pp. 6723-6728, Aug. 2024.
[93] Y. -L. Chang and Q. -X. Chu, "Broadband dual-polarized electromagnetic transparent antenna for cross-band scattering suppression," *IEEE Antennas Wireless Propag. Lett.*, vol. 21, no. 7, pp. 1452-1456, Jul. 2022.
[94] Y. Jia, H. Zhai, J. Yin, Y. Wang, and Y. Liu, "A quadruple-band shared-aperture antenna array with multiband radiation pattern restorations," *IEEE Trans. Antennas Propag.*, vol. 72, no. 10, pp. 7722-7735, Oct. 2024.
[95] Yi He, Gengming Wei, Can Ding, and Y. Jay Guo, "A new buffering scheme for collocated/shared-aperture dual-band base station antenna array utilizing tight-coupling concept," *IEEE Transactions on Antennas and Propagation*, 2025. doi: 10.1109/TAP.2025.3540554.
[96] J. P. Jacobs, "Accurate modeling by convolutional neural-network regression of resonant frequencies of dual-band pixelated microstrip antenna," *IEEE Antennas Wireless Propag. Lett.*, vol. 20, no. 12, pp. 2417–2421, 2021.
[97] S. Koziel, N. Çalık, P. Mahouti, and M. A. Belen, "Accurate modeling of antenna structures by means of domain confinement and pyramidal deep neural networks," *IEEE Trans. Antennas Propag.,* vol. 70, no. 3, pp. 2174-2188, Mar. 2022.
[98] M. C. D. Melo, P. B. Santos, E. Faustino, C. J. A. Bastos-Filho, and A. Cerqueira Sodré, "Computational intelligence-based methodology for antenna development," *IEEE Access,* vol. 10, pp. 1860–1870, 2021.
[99] Q. Wu, H. Wang, and W. Hong, "Multistage collaborative machine learning and its application to antenna modeling and optimization," *IEEE Trans. Antennas Propag.,* vol. 68, no. 5, pp. 3397–3409, May 2020.
[100] L.-Y. Xiao, W. Shao, F.-L. Jin, B.-Z. Wang, and Q. H. Liu, "Inverse artificial neural network for multiobjective antenna design," *IEEE Trans. Antennas Propag.,* vol. 69, no. 10, pp. 6651–6659, Oct. 2021.
[101] Z. Zhao, H. Zhao, Z. Wang, M. Zheng, and Q. Xun, "Radial basis function neural network optimal modeling for phase-only array pattern nulling," *IEEE Trans. Antennas Propag.*, vol. 69, no. 11, pp. 7971–7975, Nov. 2021.
[102] X. Yang, F. Yang, Y. Chen, J. Hu, and S. Yang, "Real-time pattern synthesis for large-Scale conformal arrays based on interpolation and artificial neural network method," *IEEE Trans. Antennas Propag.*, vol. 71, no. 12, pp. 9559–9570, Dec. 2023.
[103] C. Cui, W. T. Li, X. T. Ye, Y. Q. Hei, P. Rocca, and X. W. Shi, "Synthesis of mask-constrained pattern-reconfigurable nonuniformly spaced linear arrays using artificial neural networks," *IEEE Trans. Antennas Propag.*, vol. 70, no. 6, pp. 4355–4368, Jun. 2022.
[104] C. A. Guo, Q Cheng, and J. Yuan, "Multibeam Tracking for Future Multi-User Communications Employed Generalized Joined Coupler Matrix," presented as the 17th International Conference on Signal Processing and Communication System, Gold Coast, Dec. 2024.
[105] P. Mahouti, M. A. Belen, N. Calik, and S. Koziel, "Computationally efficient surrogate-assisted design of pyramidal-shaped 3-D reflectarray antennas," *IEEE Trans. Antennas Propag.*, vol. 70, no. 11 pp. 10777–10786, Nov. 2022.
[106] L. Yuan, L. Wang, X.-S. Yang, H. Huang, and B.-Z. Wang, "An efficient artificial neural network model for inverse design of metasurfaces," *IEEE Antennas Wireless Propag. Lett.*, vol. 20, no. 6, pp. 1013–1017, 2021.
[107] H. Xia, S.-L. Chen, Y. Wang, Y. Zhao, H. Jia, R. Yang, and Y. J. Guo, "Deep-learning-assisted intelligent design of terahertz hybrid-functional metasurfaces with freeform patterns," *Opt. Laser Technol.*, vol. 181, pp. 112041, Oct. 2024.
[108] P. Liu, L. Chen, and Z. N. Chen, "Prior-knowledge-guided deep-learning-enabled synthesis for broadband and large phase shift range metacells in metalens antenna," *IEEE Trans. Antennas Propag.*, vol. 70, no. 7, pp. 5024–5034, Jul. 2022.
[109] P. Naseri and S. V. Hum, "A generative machine learning-based approach for inverse design of multilayer metasurfaces," *IEEE Trans. Antennas Propag.*, vol. 69, no. 9, pp. 5725–5739, Sep. 2021.
[110] M. Li, S.-L. Chen, Y. Liu, and Y. J. Guo, "Wide-angle beam scanning phased array antennas: A review," *IEEE Open J. Antennas Propag.,* vol. 4, pp. 695-712, 2023.
[111] Y. J. Guo, *Advances in Mobile Radio Access Networks*. Norwood, MA, USA: Artech House, 2004.

Y. Jay Guo (Fellow, IEEE) received a Bachelor's Degree and a Master's Degree from Xidian University in 1982 and 1984, respectively, and a Ph.D Degree from Xian Jiaotong University in 1987. He has published six books and over 700 research papers, and he holds 27 international patents. His current research interests include 6G antennas, integrated sensing and communications systems and as well as big data technologies such as ML and digital twins.

Jay is a Fellow of the Australian Academy of Engineering and Technology, Royal Society of New South Wales and IEEE. He has won a number of the most prestigious Australian national awards. Together with his students and postdocs, he has won numerous best paper awards. He was a recipient of the prestigious 2023 IEEE APS Sergei A. Schelkunoff Transactions Paper Prize Award.

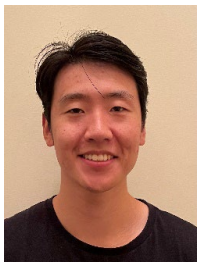

Charles A. Guo (Student Member, IEEE) received the bachelor's degree (Hons.) in advanced science from the University of Sydney in 2018, and the M.Res. degree in physics from the University of New South Wales in 2021, where he completed his Ph.D in Feb 2025. He has been employed as a part-time machine learning (ML) Research Engineer at the University of Technology Sydney since 2017, working on a number of industrial projects. His current research interests include machine learning, artificial intelligence, signal and image processing, and future wireless sensing and communications systems.

Charles was a recipient of the prestigious 2023 IEEE Sergei A. Schelkunoff Transactions Prize Paper Award.

Ming Li (Member, IEEE) received the B.S. degree and the M.S. degree from Xiamen University, Xiamen, China, in 2015 and 2018, respectively, and the Ph.D. degree from the University of Technology Sydney (UTS), Ultimo, NSW, Australia, in 2023.

Since September 2023, he has been a Post-Doctoral Research Associate with the Global Big Data Technologies Centre (GBDTC), UTS. His research interests include antenna array synthesis, and multibeam antennas.

Dr. Li was a recipient of the First Prize of Student Paper at the *ACES-China 2021*, Chengdu, China, the Best Paper Award at the *NCANT 2021,* Ningbo, China, and the Honorable Mention at the *IEEE AP-S/URSI 2022,* Denver, USA.

Matti Latva-aho (Fellow, IEEE) is a distinguished expert in wireless communications, holding M.Sc., Lic.Tech., and Dr.Tech. (Hons.) degrees in Electrical Engineering from the University of Oulu, Finland, awarded in 1992, 1996, and 1998, respectively. From 1992 to 1993, he worked as a Research Engineer at Nokia Mobile Phones in Oulu, before joining the Centre for Wireless Communications (CWC) at the University of Oulu. Prof. Latva-aho served as the Director of CWC from 1998 to 2006 and later as Head of the Department of Communication Engineering until August 2014. Currently, he is a Professor of Wireless Communications at the University of Oulu and serves as the Director of the National 6G Flagship Programme. He is also a Global Fellow at The University of Tokyo, reflecting his international recognition in the field. With an extensive portfolio of over 600 conference and journal publications, Prof. Latva-aho has significantly advanced the field of wireless communications. His contributions were recognized in 2015 when he received the prestigious Nokia Foundation Award for his groundbreaking research in mobile communications.